Available online at www.sciencedirect.com
ScienceDirect
Journal of the European Ceramic Society 30 (2010) 2977–2983
www.elsevier.com/locate/jeurceramsoc

The effect of temperature on the pulsed current processing behaviour and structural characteristics of porous ZSM-5 and zeolite Y monoliths

Petr Olegovich Vasiliev [a,b], Arto Ojuva [a], Jekabs Grins [a], Lennart Bergström [a,*]

[a] *Department of Materials and Environmental Chemistry, Arrhenius Laboratory, Stockholm University, Stockholm SE-106 91, Sweden*
[b] *EXSELENT- Berzelii Centre on Porous Materials at Stockholm University, Sweden*

Available online 5 March 2010

Abstract

Hierachically porous monoliths of ZSM-5 and Y zeolites have been prepared by pulsed current processing (PCP). The densification behaviour and structural characteristics during rapid thermal treatment of the zeolites have been determined and related to the influence of the Si:Al ratio on the thermal stability of the zeolites. Monoliths of macroscopic shape can be prepared with an insignificant loss of surface area and micropore volume when the PCP-treatment was performed at temperatures below a critical maximum PCP temperature (T_{PCP}). Full-profile fittings of the powder X-ray diffraction patterns showed that the lattice strain of zeolite Y increases rapidly above the critical T_{PCP} while the ZSM-5 zeolites undergo a phase transition from orthorhombic to monoclinic. The use of a novel ceramic processing route for the production of the zeolite monoliths that do not significantly influence the structural characteristics and surface area of the starting materials has a potential to be of importance in catalysis and gas separation applications.

Keywords: Pulsed current processing; Porosity; X-ray methods

1. Introduction

Crystalline microporous materials, e.g. zeolites, are characterized by a high surface area and a specific pore structure that defines the accessibility to the pore cavities. The pore size and pore accessibility, together with the chemistry of the active sites on the pore walls, determine the specific physicochemical properties, of importance in e.g. catalytic, ion-exchange, separation, and sorption applications.[1,2]

Zeolite Y and ZSM-5 are two of the most frequently used zeolites in catalysis. The zeolite Y structure has spherical cages which are connected tetrahedrally with four neighbouring cages by windows, thus forming a three-dimensional 12-membered-ring open pore system.[3] The aluminosilicate ZSM-5 zeolite have intersecting systems of 10-membered-ring straight and zig-zag pores. ZSM-5 is commonly used in the isomerisation of xylenes and the disproportionation of toluene.[4,5]

The use of zeolites in industrial applications usually requires that the primary zeolite powders are assembled into macroscopic secondary structures or monoliths of various shapes, e.g. cylinders and discs.[4,6,7] Many applications, e.g. catalysis and gas separation, also put other demands on the materials, e.g. high surface area, low pressure drop and a high strength, which calls for hierarchically porous materials.[8]

The current technology for producing zeolite pellets or other types of secondary structures for catalytic and adsorption applications involves extrusion or pressing zeolite particles together with a non-zeolitic binder, followed by solvent removal and heating to relatively low temperatures.[7] The risk of temperature-induced structural changes, e.g. phase transformations and pore collapse typically limit the maximum temperature. However, the strength and attrition resistance of the pellets may be rather low and the use of non-zeolitic additives will reduce the surface area and may even result in unwanted side reactions.

Several attempts to minimize or eliminate the use of non-zeolitic binders have been reported. Bowes showed how a self-bound zeolite could be prepared from an alkaline solution of silica.[9] Different zeolites prepared following this procedure showed almost an order of magnitude reduced aging rates in catalytic dewaxing processes, and side reactions catalyzed by the binder were eliminated.[10] Recently, zeolite-bound zeolite catalysts have been prepared by hydrothermal transformation of a non-zeolitic binder by using zeolite seeds.[11]

* Corresponding author. Tel.: +46 8 162368; fax: +46 8 152187.
E-mail address: lennart.bergstrom@mmk.su.se (L. Bergström).

0955-2219/$ – see front matter © 2010 Elsevier Ltd. All rights reserved.
doi:10.1016/j.jeurceramsoc.2010.02.007

We have recently shown how mechanically stable porous monoliths can be produced by pulsed current processing (PCP) of porous powders of diatomite[12] and mesoporous silica.[13] The consolidation process is restricted to the initial stage, where mass transport is insignificant and the pores inside the used material are preserved. Pulsed current processing (PCP) offers the advantages of a high heating rate, which makes the total heating time short, and the possibility of simultaneously subjecting the powder assembly to a compressive stress.

There has been a large interest in electric current-driven heating and sintering processes during the last two decades.[14,15] The detailed understanding of the process is still a topic of intense debate.[14,16–18] Various commercial manufacturers try to advertise their machines with specific trade names for the process, e.g. "plasma assisted sintering" (PAS), "Field assisted sintering technique" (FAST), and "spark plasma sintering" (SPS). We prefer to use the more neutral term "pulsed current processing" (PCP) that solely relates to the process without indicating a specific brand of machine or an assumption about the nature of the process.

In this study, we show that it is possible to produce hierarchically porous monoliths from ZSM-5 and zeolite Y powders by pulsed current processing. The temperature dependence of the densification behaviour is investigated in detail. The changes in lattice strain and unit cell parameters with PCP-treatment temperature were evaluated by a full-profile fitting procedure of the powder X-ray diffraction patterns. The temperature window within which the monoliths can be produced without structural collapse or significant loss of the surface area or micropore volume is identified and related to the influence of the SiO_2:Al_2O_3 ratio on the thermal stability of the zeolites.

2. Experimentals

2.1. Materials

ZSM-5 zeolites with SiO_2/Al_2O_3 ratios of 30 and 50, and zeolite Y with SiO_2/Al_2O_3 ratios of 30 and 60 were acquired from Zeolyst International (Conshohocken, USA).

2.2. Methods

The zeolite powders were loaded in cylindrical graphite dies (diameter 12 mm) and treated in vacuum, with an applied uniaxial pressure of 20 MPa and a heating rate of about 100 °C/min, using a pulsed current processing apparatus (Dr. Sinter 2050, Sumitomo Coal Mining Co. Ltd., Japan). The powder assemblies were treated in the pulsed current processing apparatus up to maximum temperatures (T_{PCP}) at 50° intervals between 600 °C and 1000 °C and held at these temperatures for 3 min. The temperature was monitored by a *K*-type thermocouple inserted in the graphite die. The densification of the zeolite assemblies in the axial direction was monitored by following the position of the plunger, which gives the volume and the density, using the initial sample weight, of the powder assembly.

A JEOL JSM-7000F scanning electron microscope (SEM) was used to study zeolite powders, thinly spread onto a carbon film supported on an aluminium brass stud, and zeolite monolith fracture surfaces.

Powder X-ray diffraction (PXRD) patterns were recorded using a PANalytical X′pert PRO MPD diffractometer equipped with a Pixel detector and using a Cu $K\alpha_1$ radiation source. The measurements were carried out using 16 mm diameter reflection mode holders, variable slits with a constant area of 1 cm^2 irradiated, a continuous scan mode with step size 0.0131°, the 2θ range 7–100° (a total number of 7147 points) and a total measuring time of 144 min, yielding patterns with maximum peak intensities of *ca*. 10,000. The PCP-treated materials were ground into a fine powder prior to PXRD measurements.

Full-profile fitting (Rietveld) was for ZSM-5 zeolite powders performed using the monoclinic space group $P2_1/n$ and atomic coordinates taken from the single crystal structure determination of ZSM-5, $[H_{0.32}][Si_{95.68}Al_{0.32}O_{192}]$ ($a = 1.9879$ nm, $b = 2.0107$ nm, $c = 1.3269$ nm, and $\beta = 90.67°$) by van Koningsveld et al.[19] For zeolite Y, with cubic space group Fd-3m symmetry, the atomic coordinates were taken from the database of the International Zeolite Association. Lattice strain analysis from X-ray powder diffraction peak broadenings[20,21] was performed with the Rietveld method using the program FullProf.[22] For the analysis of strain, the Thomson-Cox-Hastings pseudo-Voigt function was used, having Lorentzian and Gaussian component peak half-widths of respectively $H_L = X\tan(\theta) + Y/\cos(\theta)$ and $H_G^2 = U\tan^2(\theta) + V\tan(\theta) + W + I_G/\cos^2(\theta)$, and assuming that strain broadening is described by the terms having a $\tan(\theta)$ dependency, *i.e.* X and $U^{1/2}$. Lorentzian and Gaussian components for the instrumental resolution were estimated by measurements on a sintered NIST standard alumina disc, giving peaks with a Gaussian component above 85% and half-widths of respectively *ca*. 0.05° and 0.10° at 20° and 100°.

Nitrogen sorption data were recorded using a Micromeritics ASAP 2020 analyzer. The PCP-treated cylindrical samples, divided into four equal parts, and as-received powders were degassed at 300 °C for 5 h and adsorption and desorption data were collected at −196 °C. The specific surface areas were calculated using the Brunauer-Emmett-Teller (BET) model in the relative pressure region of 0.05–0.15 p/p_o.

The as-received zeolite powders parameters: surface areas, unit cell parameters and unit cell volumes, and full-profile fitting parameters are summarized in Table 1.

3. Results and discussion

The pulsed current processing (PCP) technique was used to produce hierarchically porous monoliths from ZSM-5 and zeolite Y powders with different SiO_2:Al_2O_3 ratios. The SEM images in Fig. 1 shows that the as-received ZSM-5 powder particles are polydisperse, having sub-micron sizes and an irregular morphology, while the zeolite Y grains are larger, about 1 μm, and have plate-like shapes.

The densification of the zeolite monoliths was followed by monitoring the position of the plunger as a function of temperature (and time) in the PCP machine. The corresponding

Table 1
Unit cell, Rietveld refinement, and surface area data for as-received ZSM-5 and Y powders.

Sample	ZSM-5(30)	ZSM-5(50)	Zeolite Y(30)	Zeolite Y(60)
Space group	Pnma	Pnma	Fd-3m	Fd-3m
a (nm)	1.9942(2)	1.9926(2)	2.4281(1)	2.4314(1)
b (nm)	2.0126(2)	2.0109(2)		
c (nm)	1.3436(1)	1.3412(1)		
V (nm^3)	5.392	5.374	14.321	14.374
Strain$_0$ (%)	0.11(1)	0.12(1)	0.10(1)	0.13(1)
Specific surface area, S (m^2/g)	389	401	827	853
R_F (%)	5.1	4.9	6.1	6.0
R_p (%)	15.8	14.8	13.4	13.4
R_{wp} (%)	18.7	17.4	13.7	13.8
χ^2	4.2	3.8	2.3	2.4

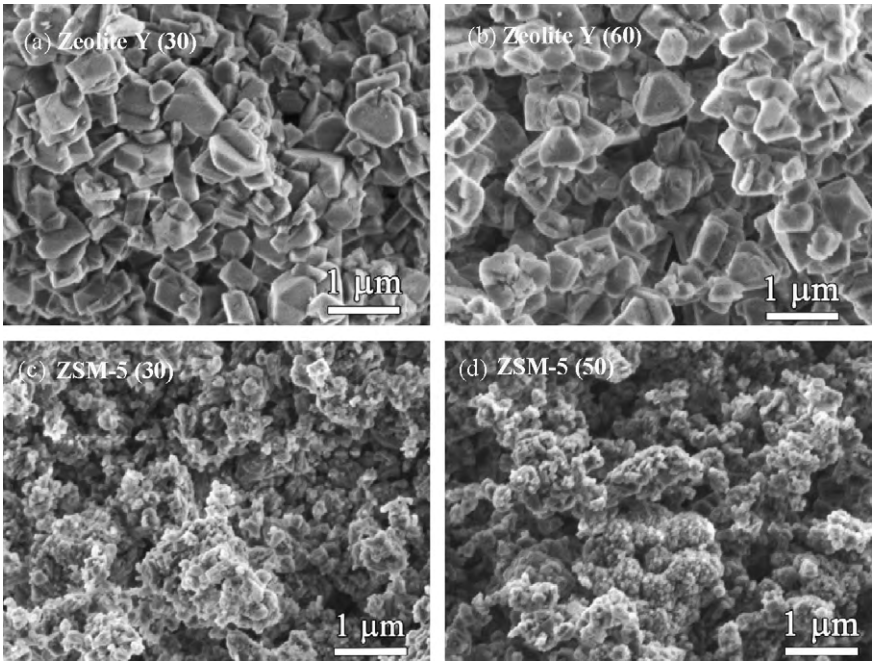

Fig. 1. Scanning electron micrographs of the as-received zeolite powders: (a) zeolite Y(30); (b) zeolite Y(60); (c) ZSM-5(30); (d) ZSM-5(50).

specific density of the powder body was calculated using the initial weight of the sample. In Fig. 2, the observed densification rates during PCP, dρ/dt [kg/m^3 s] with ρ being the density of the sample, is shown as a function of temperature. Fig. 2 clearly shows that all the zeolites can be characterized by a relatively narrow temperature range within which there is a large increase of the densification rate. For ZSM-5 zeolites, the densification rate rapidly increases from 0.1 kg/m^3 s to 0.7 kg/m^3 s in the temperature range of 800–1000 °C, for zeolite Y(30) dρ/dt increases from 0.1 kg/m^3 s to 1.0 kg/m^3 s between 750 °C and

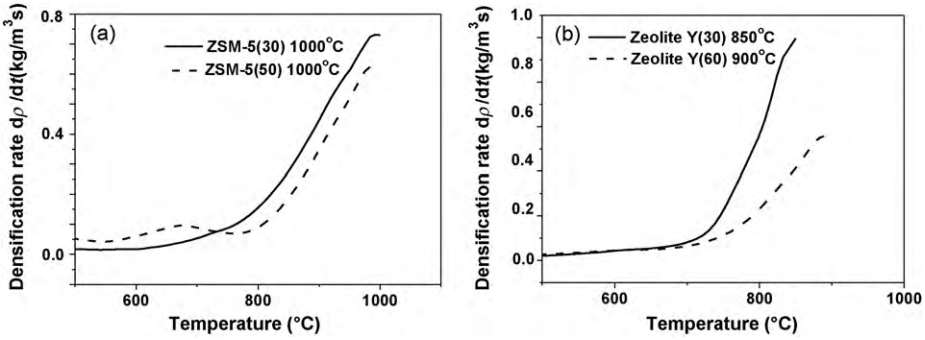

Fig. 2. Densification rate as a function of temperature during pulsed current processing for four different zeolite powders: (a) ZSM-5(30) and ZSM-5(50), (b) Zeolite Y(30) and Zeolite Y(60). ρ corresponds to density and t corresponds to time. The heating rate for each sample was 100 °C/min.

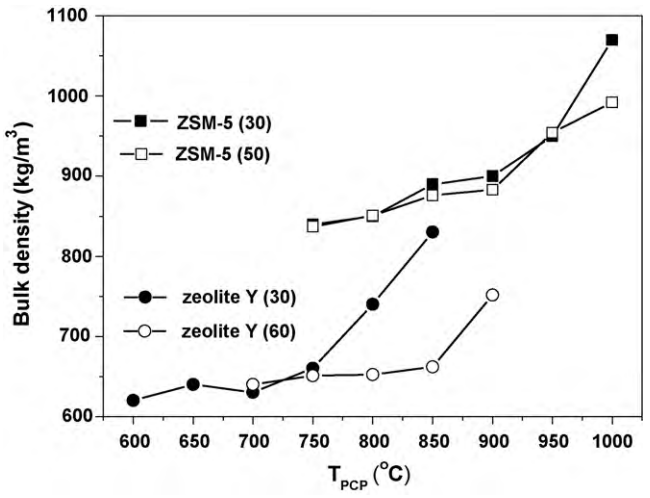

Fig. 3. Bulk density as a function of the maximum PCP temperature (T_{PCP}) for the zeolite powder bodies have been subjected to during pulsed current processing.

850 °C, and for zeolite Y(60) the densification rate increases from 0.1 kg/m^3 s to 0.6 kg/m^3 s in the temperature range of 800–900 °C.

Fig. 3 shows how the bulk densities of the compacted powder bodies, estimated from the mass of the powder and dimensions of the processed monoliths, vary with T_{PCP}. The ZSM-5 zeolites do not show any significant difference in consolidation behaviour for the materials with different Al-contents. The zeolite Y materials, however, display a densification behaviour that depend on the Si:Al ratio; the zeolite Y(30) powder displays a significant densification at about 750 °C while the zeolite Y(60) powder, with a comparatively lower Al-content, densifies at a significantly higher temperature, around 850 °C. This difference in densification behaviour with temperature corroborates the observed temperature dependence of the densification rate shown in Fig. 2.

Fig. 4 shows how the gas uptake is modified by the PCP-treatment of the zeolites. The as-received powders display a significant nitrogen gas uptake at low relative pressures, typical for microporous materials, and a minor hysteresis loop at a relative pressure range of 0.65–0.99 for ZSM-5(30) (Fig. 4a) and 0.48–0.99 for ZSM-5(50) (Fig. 4b) respectively, that can be related to the larger interparticle pores.

Fig. 4a shows that PCP-treatment at a T_{PCP} at 800 °C has an insignificant influence on the characteristics of the isotherms and the total gas uptake of ZSM-5(30). PCP-treatment at a T_{PCP} of 1000 °C, however, results in a significant decrease of the gas uptake while the overall shape of the isotherms is preserved. The isotherms for ZSM-5(50) (Fig. 4b) show that pulsed current processing at T_{PCP} below 900 °C result in only a minor reduction of the nitrogen uptake. The PCP-treatment induces a hysteresis step in the low-relative pressure range of 0.15–0.3 for both the PCP-treated ZSM-5 materials, but more pronounced for the ZSM-5(50). This hysteresis step is not completely understood, but it is probably associated with a phase transition from a disordered nitrogen adsorbate state to a more ordered nitrogen adsorbate state.[24,25]

The nitrogen sorption isotherms for the PCP-treated zeolite Y materials, Fig. 4c and d, provide further support that the zeolite Y(60) material with a lower Al-content can sus-

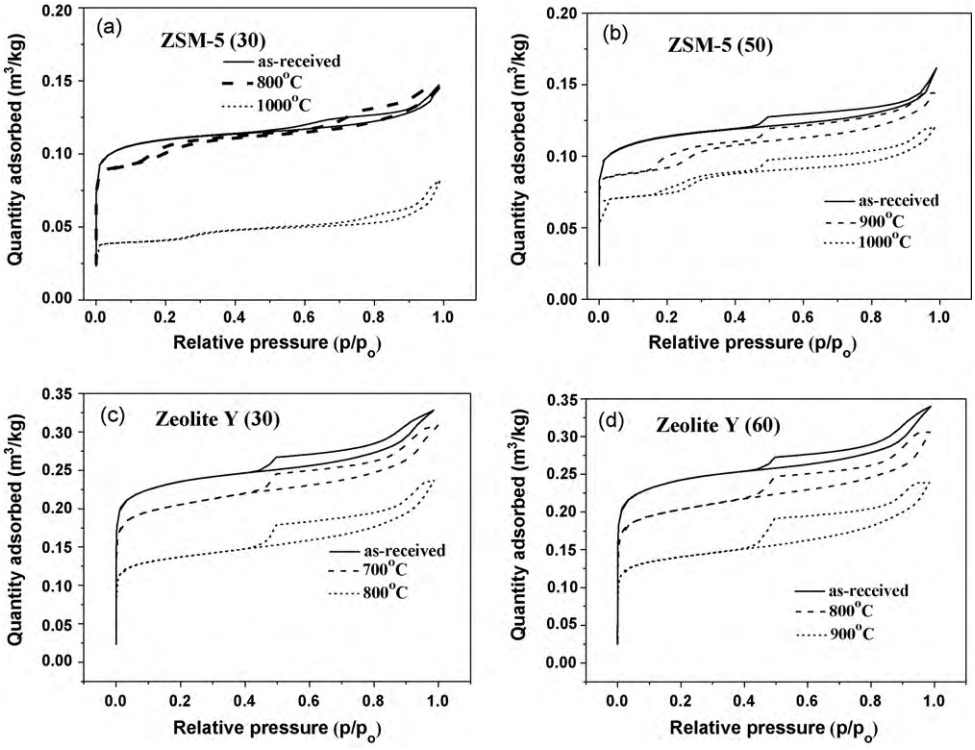

Fig. 4. Nitrogen sorption isotherms for zeolites: (a) ZSM-5(30); (b) ZSM-5(50); (c) Y(30); (d) Y(60). The isotherms for the as-received powders are compared with the materials that have been PCP-treated at different T_{PCP}.

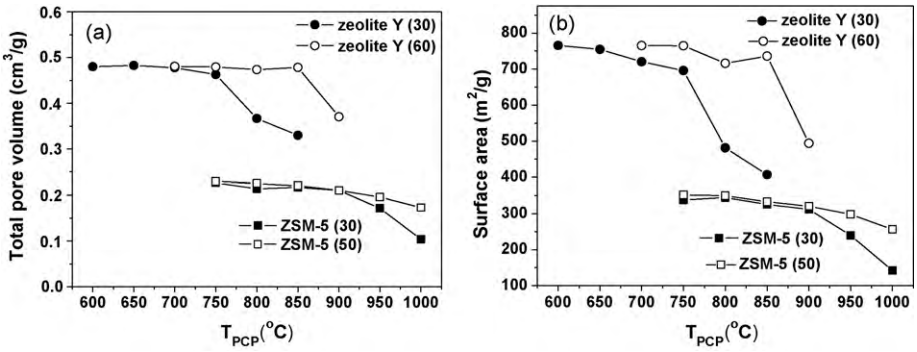

Fig. 5. The effect of the maximum PCP temperature (T_{PCP}) on the: (a) total pore volume and (b) specific surface area of four different zeolites.

tain PCP-treatment at a higher T_{PCP} compared to the zeolite Y(30) material without a significant decrease of the gas uptake.

Fig. 5 shows that it is possible to identify a critical T_{PCP} for each zeolite above which the pore volume and the specific surface area decrease significantly. The two ZSM-5 materials display a negligible decrease of the pore volume and maintain 80% or more of the surface area compared to the as-received powders at a T_{PCP} below 900 °C. Fig. 5 also shows that the zeolite Y monoliths are thermally less stable compared to the ZSM-5 monoliths. The temperature dependence shown in the nitrogen sorption data correspond well with the densification behaviour and can be associated with a significant collapse of the micropores at temperatures above the critical T_{PCP}, which is characteristic for each specific zeolite.[23] The difference in pore stability for the two different zeolite Y materials, of about 100 °C, can be attributed to the dependence of the thermal stability on the Al-content.[26]

The structural changes in the zeolite powders processed at different T_{PCP} were characterized by PXRD by determining the unit cell volumes and lattice strain using the Rietveld method. As shown in Fig. 6, the lattice strain increases rapidly above 750 °C for zeolite Y(30) and above 850 °C for zeolite Y(60). The calculated lattice strain of ZSM-5 (Fig. 6(b)) shows a continuous increase, relative to that in the as-received material, with increasing T_{PCP}. The lattice strain of zeolite Y shows a stronger dependence on T_{PCP} than ZSM-5. The observed increases in lattice strain probably reflect the degree to which the PCP and the accompanying amorphization cause a deformation of the structure. Previous studies of various zeolite powders shows that an amorphization of the crystalline zeolitic structure can be induced by different treatments, e.g. by heating, ball milling or applying a pressure.[27,28]

The as-received ZSM-5 zeolites have an orthorhombic structure (space group Pnma), while the PCP-treated ZSM-5 samples were found to be monoclinic (space group $P2_1/n$).[19] This is in agreement with previous findings that synthetic MFI type zeolites can transform from orthorhombic to monoclinic with minor displacements of atomic positions.[29–31] The monoclinic β angle was found to be nearly constant, *ca.* 90.45° (not shown), while the lengths of the unit cell axes all decreased with increasing T_{PCP}. Fig. 7 shows how the unit cell volume decreases with increasing T_{PCP} and that the decrease is larger for ZSM-5(30) than for ZSM-5(50). The PCP-treatment of zeolite Y powders induces a uniform contraction of the cubic unit cell volume, as shown in Fig. 7. The observed decrease in unit cell volume with increasing T_{PCP} is probably related to the build-up of lattice strain (Fig. 6) by the PCP-treatment.

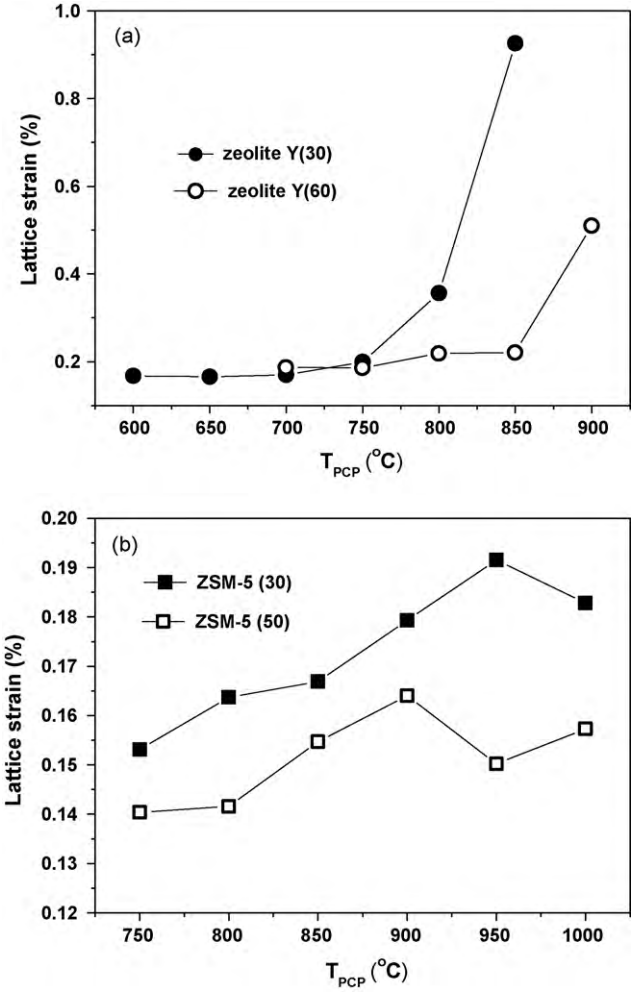

Fig. 6. Lattice strain as a function of T_{PCP} for zeolites: (a) Y(30) and Y(60) and (b) ZSM-5(30) and ZSM-5(50).

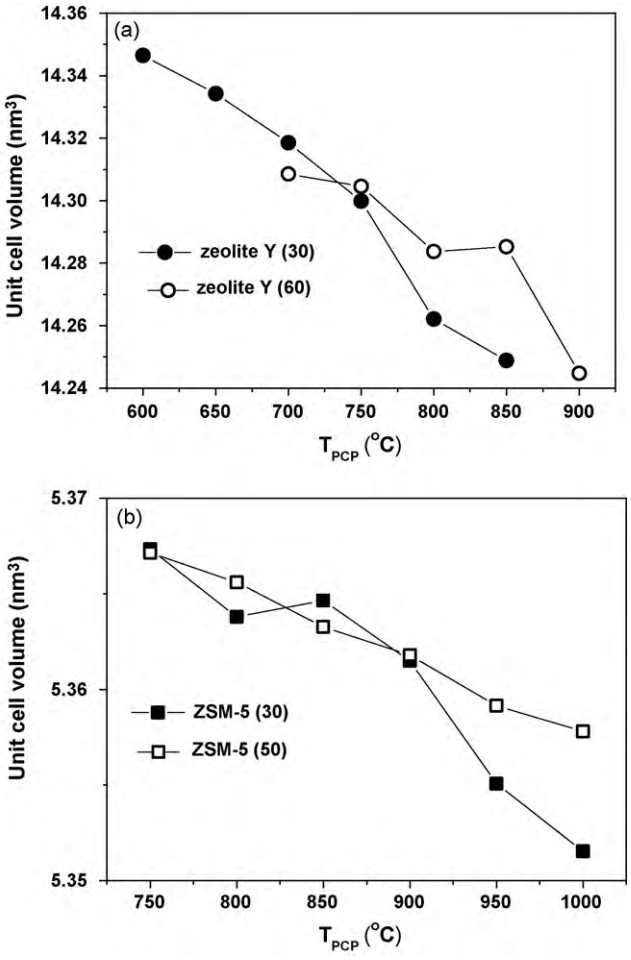

Fig. 7. Unit cell volume as a function of T_{PCP} for zeolites: (a) Y(30) and Y(60) and (b) ZSM-5(30) and ZSM-5(50).

4. Summary

Zeolite monoliths have been produced from zeolite ZSM-5 (SiO_2/Al_2O_3 ratios of 30 and 50) and from zeolite Y (SiO_2/Al_2O_3 ratios of 30 and 60) by pulsed current processing (PCP). Restricting the PCP maximum temperature to the critical temperature ranges of 700–750 °C for zeolite Y(30), 800–850 °C for zeolite Y(60), 850–900 °C for ZSM-5(30) and 900–950 °C for ZSM-5(50), result in mechanically stable monoliths with a multimodal porosity, where the microporosity and crystal structure of the zeolites are virtually unaffected by the heating process. Rietveld analysis of the powder X-ray diffraction data shows that the PCP processing induces a lattice strain in the materials. The possibility to tune the porosity and density of hierarchically porous zeolite monoliths may find applications where the combination of mechanical stability and zeolitic properties (selectivity, acidity) are of high importance, e.g. in catalysis and gas separation.

Acknowledgements

This work was performed within the Berzelii centre EXSELENT on porous materials supported by VINNOVA and VR. We thank Prof. Mats Nygren, Dr. Kjell Jansson, Doc. Niklas Hedin for their advice and assistance during this work.

References

1. Breck DW. *Zeolite molecular sieves: structure, chemistry, and use*. New York: John Wiley & Sons Inc.; 1984.
2. Weitkamp J, Puppe L. *Catalysis and zeolites: fundamentals and applications*. Berlin, Heidelberg: Springer-Verlag; 1999.
3. Breck DW. *Zeolite molecular sieves: structure, chemistry and use*. New York: John Wiley & Sons Inc.; 1974.
4. Sherman JD. Synthetic zeolites and other microporous oxide molecular sieves. *Proc Natl Acad Sci USA* 1999;**96**(7):3471–8.
5. Flanigen EM, Bennett JM, Grose RW, Cohen JP, Patton RL, Kirchner RM, et al. Silicalite, a new hydrophobic crystalline silica molecular-sieve. *Nature* 1978;**271**(5645):512–6.
6. Crittenden B, Thomas WJ. *Adsorption technology and design*. Elsevier; 1998.
7. Satterfield CN. *Heterogeneous catalysis in industrial practice*. New York: Krieger Publishing Company; 1996.
8. Perez-Ramirez J, Christensen CH, Egeblad K, Christensen CH, Groen JC. Hierarchical zeolites: enhanced utilisation of microporous crystals in catalysis by advances in materials design. *Chem Soc Rev* 2008;**37**(11):2530–42.
9. Bowes, E. Extrusion of silica-rich solids. *United States Patent* 4,582,815; 1986.
10. Bowes, E. Catalytic dewaxing process using binder-free catalyst. *United States Patent* 4,872,968; 1989.
11. Rauscher M, Selvam T, Schwieger W, Freude D. Hydrothermal transformation of porous glass granules into ZSM-5 granules. *Micropor Mesopor Mat* 2004;**75**(3):195–202.
12. Akhtar F, Vasiliev PO, Bergstrom L. Hierarchically porous ceramics from diatomite powders by pulsed current processing. *J Am Ceram Soc* 2009;**92**(2):338–43.
13. Vasiliev PO, Shen ZJ, Hodgkins RP, Bergstrom L. Meso/macroporous, mechanically stable silica monoliths of complex shape by controlled fusion of mesoporous spherical particles. *Chem Mater* 2006;**18**(20):4933–8.
14. Munir ZA, Anselmi-Tamburini U, Ohyanagi M. The effect of electric field and pressure on the synthesis and consolidation of materials: a review of the spark plasma sintering method. *J Mater Sci* 2006;**41**(3):763–77.
15. Shen Z, Nygren M. Microstructural prototyping of ceramics by kinetic engineering: applications of spark plasma sintering. *Chem Rec* 2005;**5**(3):173–84.
16. Tokita M. Development of large-size ceramic/metal bulk FGM fabricated by spark plasma sintering. *Mater Sci Forum* 1999;**308–311**:83.
17. German RM. *Sintering theory and practice*. New York: Wiley; 1996.
18. Xie GQ, Ohashi O, Song MH, Mitsuishi K, Furuya K. Reduction mechanism of surface oxide films and characterization of formations on pulse electric-current sintered Al–Mg alloy powders. *Appl Surf Sci* 2005;**241**(1–2):102–6.
19. van Koningsveld H, Jansen JC, van Bekkum H. The monoclinic framework structure of zeolite H-ZSM-5. Comparison with the orthorhombic framework of as-synthesized ZSM-5. *Zeolites* 1990;**10**(4):235–42.
20. Delhez R, Keijser THD, Langford JL, Louër D, Mittemeijer EJ, Sonnefeld EJ. *Crystal imperfection broadening and peak shape in the Rietveld method*. Oxford University Press; 1993.
21. Balzar D, Audebrand N, Daymond MR, Fitch A, Hewat A, Langford JI, et al. Size-strain line-broadening analysis of the ceria round-robin sample. *J Appl Crystallogr* 2004;**37**:911–24.
22. Rodríguez-Carvajal J. Recent developments of the program FullProf. *Comm Powder Diffr (IUCr) Newslett* 2001;**26**:12–9.
23. Cruciani G. Zeolites upon heating: factors governing their thermal stability and structural changes. *J Phys Chem Solids* 2006;**67**(9–10):1973–94.
24. Mueller U, Unger KK. Sorption studies on large ZSM-5 crystals: the influence of aluminium content, the type of exchangeable cations and the temperature on nitrogen hysteresis effects. In: Unger KK, Rouquerol J, Sing KSW, Kral H, editors. *Characterization of porous solids*, vol. 39. Amsterdam: Elsevier; 1988. p. 101.

25. Li HC, Sakamoto Y, Liu Z, Ohsuna T, Terasaki O, Thommes M, et al. Mesoporous silicalite-1 zeolite crystals with unique pore shapes analogous to the morphology. *Micropor Mesopor Mat* 2007;**106**(1–3):174–9.
26. Petrovic I, Navrotsky A. Thermochemistry of Na-faujasites with varying Si/Al ratios. *Micropor Mater* 1997;**9**(1–2):1–12.
27. Greaves GN, Meneau F, Sapelkin A, Colyer LM, Gwynn IA, Wade S, et al. The rheology of collapsing zeolites amorphized by temperature and pressure. *Nat Mater* 2003;**2**(9):622–9.
28. Greaves GN, Meneau F, Kargl F, Ward D, Holliman P, Albergamo F. Zeolite collapse and polyamorphism. *J Phys Condens Matter* 2007;**19**(41).
29. van Koningsveld H, Jansen JC, van Bekkum H. The orthorhombic monoclinic transition in single-crystals of zeolite ZSM-5. *Zeolites* 1987;**7**(6):564–8.
30. Hay DG, Jaeger H, West GW. Examination of the monoclinic orthorhombic transition in silicalite using XRD and silicon NMR. *J Phys Chem* 1985;**89**(7):1070–2.
31. Wu EL, Lawton SL, Olson DH, Rohrman AC, Kokotailo GT. ZSM-5-type materials—factors affecting crystal symmetry. *J Phys Chem* 1979;**83**(21):2777–81.